

Vacancies in CdTe: Experiment and theory

S. Lany, V. Ostheimer, H. Wolf, Th. Wichert

Technische Physik, Universität des Saarlandes, 66041 Saarbrücken, Germany

Abstract

Ab initio calculations in the framework of density functional theory are employed to complement experimental PAC and EPR data on vacancies in CdTe. The Te vacancy is found to be a negative-U centre with a large lattice relaxation in the neutral and the doubly charged state. The electronic state introduced by V_{Te} lies below the valence band maximum for V_{Te}^0 and shifts to above the conduction band minimum for V_{Te}^{++} . An experimentally observed electric field gradient is interpreted in terms of acceptor compensation by V_{Te}^{++} . Experimental data available for the Cd vacancy is discussed in the context of the calculated electric field gradients. A Jahn-Teller effect for V_{Cd} is not confirmed.

PACS: 61.72.Vv, 71.55.Gs, 76.80.+y

Keywords: vacancy, CdTe, EFG, DFT

e-mail: Lany@tech-phys.uni-sb.de

1. Introduction

Besides intentionally introduced dopants and residual impurity atoms, intrinsic defects, e.g. vacancies and interstitials, can strongly influence the optical and electrical properties of semiconductors and consequently have been a subject of intense research [1, 2]. Except for the positron annihilation spectroscopy (PAS), most locally sensitive methods investigate vacancies indirectly via the hyperfine interaction (HFI) at neighbouring nuclei. In order to determine vacancy related HFI parameters, methods such as electron paramagnetic resonance (EPR), electron nuclear double resonance (ENDOR) and perturbed angular correlation spectroscopy (PAC) have been used. The correct experimental identification and characterisation of vacancies, however, is more difficult compared to the investigation of impurity atoms, which can be introduced into the semiconductor crystal by a controlled doping process, e.g. by ion implantation.

As a theoretical instrument being generally helpful to characterise dopants in semiconductors as well as intrinsic defects (e.g. Ref. [3]), the density functional theory (DFT) formalism is used in order to compensate for the particular difficulty to investigate vacancies. The DFT calculations yield defect related information that is difficult to access by experiment such as about the electronic structure and structural relaxations. Additionally, the identification of a particular defect is supported by the calculation of defect related parameters, such as the electric field gradient (EFG), which is used experimentally as a 'fingerprint' of the studied defect.

In the present work, the EFG tensor – characterised by the largest component V_{zz} and the asymmetry parameter η – is measured by PAC (for details, see e.g. Ref. [4]), using the radioactive probe nuclides ^{111}In and ^{111}Ag . In II-VI semiconductors, the $^{111}\text{In}_{\text{Cd}}$ donor and the $^{111}\text{Ag}_{\text{Cd}}$ acceptor form donor-acceptor (D-A) pairs with dopants, residual impurities or intrinsic defects, and in either case the EFG is determined at the $I = 5/2$ excited state of the daughter isotope ^{111}Cd [4]. It is emphasised that in CdTe, the daughter isotope ^{111}Cd is a host atom and consequently the measured EFG characterises the isolated defect. The absolute number of radioactive probe atoms needed for PAC measurements is 10^{11} - 10^{12} , and the resulting concentrations are generally low enough (10^{15}cm^{-3} and less) that the electrical properties of the semiconductor crystals are not changed significantly.

The DFT calculations are performed using the linearised augmented plane wave (LAPW) method implemented in the WIEN97 [5] program package. The general treatment of an impurity in a semiconductor for EFG calculation within this method is described in Ref. [6]. In addition to the 32 atom supercell in BCC structure with T_d symmetry used in that work, a 32 atom cell with C_{3v} symmetry is used in the present case of the cadmium vacancy. In the LAPW method, the basis set consists of plane waves augmented by a spherical harmonics expansion within so-called "muffin-tin" spheres around the atomic positions. In general, the wave functions are described by the plane wave basis at a vacancy site, but the use of an "empty sphere" allows an angular momentum decomposition

of the vacancy related states for analysis purposes. Magnetic hyperfine fields are not calculated in the present work.

2. The tellurium vacancy

From simple valence arguments, the tellurium vacancy V_{Te} accounts for a double donor, having an occupied a_1 level (s -like) and an unoccupied t_2 level (p -like) in the neutral state. Thus, no Jahn-Teller effect and no symmetry lowering from T_d symmetry is expected. A paramagnetic centre observed by EPR [7] and ENDOR [8] has been interpreted as V_{Te}^+ , but this assignment was questioned in Ref. [9], where calculations with the linear muffin tin orbital method in the atomic sphere approximation (LMTO-ASA) yielded HFI constants incompatible with the experimental results. Furthermore, the ENDOR data require that the electron spin is localised at the vacancy site to about 96%, which is rather implausible for a vacancy and strongly differs from the theoretical localisation of 20% of the electron spin within the ASA sphere.

Using a 32 atom cell with all neighbouring atoms of the tellurium vacancy fixed at ideal lattice positions, i.e. suppressing the relaxation, we find the a_1 level within the gap for all three charge states V_{Te}^0 , V_{Te}^+ and V_{Te}^{++} , occupied by two, one and zero electrons, respectively. The localisation of 10% of the electron (a_1 level) within the LAPW muffin-tin sphere for V_{Te}^+ compares well with the 20% for the LMTO-ASA sphere, taking into account the different volumes of the respective spheres. From the positions of the a_1 level for the three charge states with respect to the valence band maximum (VBM), the transition energies $E(+++) = E_{\text{VBM}} + 0.76$ eV and $E(+/0) = E_{\text{VBM}} + 1.22$ eV are inferred, which are in good agreement with the electron removal energies of 0.67 eV and 1.27 eV, reported in Ref. [9].

Taking into account the relaxation of nearest neighbour (NN) Cd atoms, which was not possible in the LMTO calculations, has drastic implications. With exception of V_{Te}^+ , strong relaxation occurs resulting in a shift of the energetic position of the a_1 level and a significant lowering of the total energy (see Table 1). In Fig. 1a, the total density of states (DOS) is shown for the relaxed configurations of the three charge states (note that for the unrelaxed configuration of all three charge states, the DOS resembles the DOS shown for V_{Te}^+ , except from the occupation number). In Fig. 1b, the a_1 level and the t_2 level are identified by the respective s and p character within the muffin-tin sphere at the vacancy site. Only for V_{Te}^+ , the a_1 level is still positioned within the band gap after relaxation. While for V_{Te}^0 , the strong inward relaxation of the NN-Cd atoms leads to a shift of the a_1 level to below the VBM, this level is shifted to above the conduction band minimum (CBM) during the outward relaxation in the 2+ state. The 2+ state of V_{Te} is comparable with the 3+ state of the arsenic vacancy in GaAs, which also has an *empty* a_1 level and was calculated in Ref. [10]. There, the observed outward relaxation of the NN-Ga atoms was interpreted by the authors in terms of a rehybridisation towards sp^2 bonding. A similar argument holds in the present case for V_{Te}^{++} , where the NN-Cd atoms move about 60% of their way towards a planar sp^2 bonding configuration with the NNN-Te atoms. In the neutral state of V_{Te} , the a_1 orbital is *fully occupied* and there is a pronounced p_z -like contribution within the NN-Cd spheres (the local z -axis directs towards the vacancy). Consequently, the sp^3 configuration is retained from point of view of a NN-Cd atom, causing the strong inward relaxation of the NN-Cd shell. After relaxation, the a_1 level is located 0.5 eV below the VBM (cf. Fig. 1b, left hand side). In the singly charged state V_{Te}^+ , where the a_1 level is *half occupied*, the counteracting mechanisms described for V_{Te}^0 and V_{Te}^{++} approximately cancel each other, leading to only little relaxation and energy gain (cf. Table 1).

The transition energy between two charge states measures the Fermi level E_F for which the formation energy E_{form} of both states is equal (the formation energy of charged defects depends on E_F). Accordingly, the relative formation energy ΔE_{form} with respect to V_{Te}^0 is plotted in Fig. 2a in the case of suppressed relaxation. Due to the relaxation, however, the formation energies are lowered by the respective relaxation energies ΔE_r (Fig. 2b). In fact, the large relaxation energies for V_{Te}^0 and V_{Te}^{++} (cf. Table 1) result in a negative-U behaviour with a transition energy $E(++/0) = E_{\text{VBM}} + 0.85$ eV

between V_{Te}^{++} and V_{Te}^0 , and the paramagnetic state V_{Te}^+ is never the most stable state, independent of the Fermi energy. Consequently, it should not be observed in an EPR experiment. Therefore, the rejection of the EPR identification of V_{Te}^+ in Ref. [9] is confirmed. The fact that for the calculations of the HFI constants in Ref. [9] relaxation was neglected, does not harm, because in the paramagnetic 1+ state the relaxation is quite small (cf. Table 1).

It is pointed out that the tellurium vacancy exhibits a rather extreme Franck-Condon effect, and thermal and optical excitation energies are no longer comparable. An optical excitation does not seem possible at all, because in the stable states V_{Te}^0 and V_{Te}^{++} , the a_1 level is "hidden" in the valence band and in the conduction band, respectively. According to our LAPW calculations, the negative-U effect for the Te vacancy is very strongly pronounced, so that this property should not be affected by errors that may arise from the local density approximation and the estimation of the transition energies via the level positions. The negative-U behaviour accompanied by large lattice relaxation seems to be a rather general feature of anion vacancies in II-VI semiconductors; it has been found also for V_{Se} in ZnSe [11], while the extreme shift of the a_1 level into the valence band (neutral state) and into the conduction band (2+ state) was not reported there.

In order to investigate the interaction between Ag and Cu dopants, 2 nm copper were evaporated onto a CdTe crystal implanted with ^{111}Ag ions. After subsequent annealing at 500 K, PAC measurements yield an EFG of $V_{zz} = \pm 22.8(9) \cdot 10^{21} \text{ V/m}^2$ with $\eta = 0.0(3)$ ($T_M = 295 \text{ K}$). This value, which is unusually high for an EFG measured at the ^{111}Cd nucleus in CdTe, is close to the calculated EFG at a NN-Cd site for V_{Te}^{++} , $V_{zz} = +24.6 \cdot 10^{21} \text{ V/m}^2$ with $\eta = 0$ (see Table 1). Based on EFG calculations for interstitial Ag in CdTe, it is not expected that the interaction of ^{111}Ag with Cu atoms, e.g. the formation of $^{111}\text{Ag}_{\text{Cd}}\text{-Cu}_i$ pairs, would result in the observation of such a strong EFG. Therefore, the observed EFG is interpreted with the formation of close $^{111}\text{Ag}_{\text{Cd}}\text{-V}_{\text{Te}}^{++}$ pairs and shows the capability of the Te vacancy to compensate group I acceptors.

3. The cadmium vacancy

After the D-A pair formation of ^{111}In donors with the double acceptor V_{Cd} , the PAC probe is a NNN-atom with respect to the defect causing the EFG. Three distinct EFG have been reported in literature for the $^{111}\text{Cd}\text{-V}_{\text{Cd}}$ pair: One, labelled EFG1 in the following (values are given in Table 2), is observed after annealing ^{111}In doped CdTe under tellurium vapour pressure [12, 13]. A set of two EFG, EFG2 and EFG3, is observed simultaneously in crystals doped additionally with stable In to a level higher than 10^{18} cm^{-3} [14]. Similar EFG have been reported for ternary $\text{Hg}_{0.05}\text{Cd}_{0.95}\text{Te}$ compounds [15]. The stronger EFG, EFG2 and EFG3, which are observed when a background donor doping level is present, have been discussed in Refs. [14] and [15] in terms of a different charge state of V_{Cd} and the possibility that two In donors (one stable In atom and one ^{111}In isotope) bind to the double acceptor V_{Cd} . The LAPW calculations, using a 32 atom supercell in T_d symmetry containing a Cd vacancy, yield an atomic relaxation ($\Delta d_{\text{NN}} \approx -13\%$) which is less pronounced than in the case of V_{Te} and essentially independent of the charge state. In Table 2, the experimentally observed EFG are compared to the EFG calculated for the NNN-Cd site: Assigning EFG1, EFG2, and EFG3 to the neutral, singly, and doubly charged Cd vacancy, respectively, yields a relatively good agreement between experimental and theoretical data. It is noted, however, that in the 32 atom supercell, only three of the four Te neighbours to the Cd probe are contained within the supercell and a larger cell should be used. First calculations with a 64 atom supercell are currently running, indicating changes in the calculated EFG that are not very large, but significant. Therefore, the assignment of EFG1, EFG2, and EFG3 to the three charge states of V_{Cd} is only tentatively at the present, and the possibility that two In atoms bind to V_{Cd} can not be excluded.

In the simple orbital model, the neutral cadmium vacancy has a fully occupied a_1 level and a t_2 level, which is partly occupied by four electrons. In principle, V_{Cd}^0 and the paramagnetic state V_{Cd}^- can be subject to a Jahn-Teller effect due to the partial occupation of the t_2 level. In this case, the t_2 orbital

(*p*-like) would split into an occupied *e* level (*p_{xy}*-like) and an unoccupied (V_{Cd}^0) or half occupied (V_{Cd}^-) upper a_1 level (*p_z*-like), accompanied by a symmetry lowering from T_d to C_{3v} ; i.e. one NN-Te atom would relax stronger towards the vacancy site than the others (cf. Ref. [16], where V_{Zn} in ZnSe is discussed). An EPR signal, presenting trigonal symmetry, has been interpreted as resulting from V_{Cd}^- in a Jahn-Teller distorted configuration with the hole localised at one Te neighbour [17]. In order to investigate the Jahn-Teller effect theoretically, calculations with a 32 atom supercell in C_{3v} symmetry were performed. The interesting result is that the calculated forces on the NN-Te atoms tend to restore deviations from T_d symmetry for both the neutral and the singly charged state. Even for a strong trigonal distortion, no single, unoccupied band (the upper a_1 level, containing the holes localised at one Te neighbour) would separate from the valence band in the case of V_{Cd}^0 , as expected in the presence of a Jahn-Teller effect. Rather the holes occupy valence band like states and are moderately localised at the NN-Te shell (6% within each muffin-tin sphere of the NN-Te atoms). Thus, the DFT calculations clearly disagree with the assumption of a Jahn-Teller effect. It is further noted that in case of a Jahn-Teller distortion, the NNN-Cd atoms are no longer equivalent, and a set of three EFG instead of a single one should be observed for both the neutral and the singly charged state of V_{Cd} . This behaviour is not reflected by the PAC experiments. The discrepancies regarding the Jahn-Teller effect and the different possible interpretations of the experimentally observed EFG show that the cadmium vacancy still deserves further investigation.

4. Summary and outlook

DFT calculations of the tellurium vacancy in CdTe give access to the complex behaviour of this defect regarding the lattice relaxation and the electron structure which both change drastically with the charge state. Thus, a negative-U behaviour of V_{Te} is predicted and the paramagnetic V_{Te}^+ state should not be stable. Additionally, the acceptor compensation by doubly charged Te vacancies is discussed on the basis of the calculated EFG and experimental PAC data. As for the cadmium vacancy, the presence of a Jahn-Teller distortion is not confirmed. First calculations using a 32 atom supercell with symmetrical relaxation around the Cd vacancy yield a reasonable agreement with experimentally determined EFG, but due to the fact that the site of the probe atom is a next nearest neighbour to the vacancy, the use of a larger supercell is indicated. Calculations with a 64 atom supercell are expected to improve the detailed interpretation of the experimental data.

The financial support of the Bundesministerium für Bildung und Forschung (BMBF) under Contract No. 03WI4SAA is gratefully acknowledged.

References

- [1] *Identification of Defects in Semiconductors*, ed. M. Stavola, *Semiconductors and Semimetals* Vols. 51A and 51B, San Diego, 1999, and references therein.
- [2] G.F. Neumark, *Materials Science and Engineering R21*, (1997) 1, and references therein.
- [3] C.G. Van de Walle, D.B. Laks, G.F. Neumark, S.T. Pantelides, *Phys. Rev. B* 47 (1993) 9425.
- [4] Th. Wichert, in [1], Vol. 51B, pp. 297.
- [5] P. Blaha, K. Schwarz, J. Luitz, *WIEN97, A Full Potential Linearized Augmented Plane Wave Package for Calculating Crystal Properties* (Karlheinz Schwarz, Techn. Universität Wien, Austria), 1999. ISBN 3-9501031-0-4.
- [6] S. Lany, P. Blaha, J. Hamann, V. Ostheimer, H. Wolf, Th. Wichert, *Phys. Rev. B* 62 (2000) R2259.
- [7] B.K. Meyer, P. Omling, E. Weigel, G. Müller-Vogt, *Phys. Rev. B* 46 (1992) 15135.
- [8] D.M. Hofmann, B.K. Meyer, T. Pawlik, P. Altehheld, J.-M. Spaeth, *Mat. Sci. Forum* 143-147 (1994) 417.
- [9] M. Illgner, H. Overhof, *Phys. Rev. B* 54 (1996) 2505.
- [10] J.E. Northrup, S.B. Zhang, *Phys. Rev. B* 50 (1994) R4962.
- [11] A. García, J.E. Northrup, *Phys. Rev. Lett.* 74 (1995) 1131.
- [12] R. Kalish, M. Deicher, G. Schatz, *J. Appl. Phys.* 53 (1982) 4793.
- [13] Th. Wichert, T. Krings, H. Wolf, *Physica B* 185 (1993) 297.
- [14] T. Filz, J. Hamann, R. Müller, V. Ostheimer, H. Wolf, Th. Wichert, *J. Cryst. Growth* 159 (1996) 68.
- [15] J.C. Austin, Wm.C. Hughes, B.K. Patnaik, R. Triboulet, M.L. Swanson, *J. Appl. Phys.* 86 (1999) 3576.
- [16] G.D. Watkins, *J. Cryst. Growth* 159 (1996) 338, and references therein.
- [17] P. Emanuelsson, P. Omling, B.K. Meyer, M. Wienecke, M. Schenk, *Phys. Rev. B* 47 (1993) 15578.

Tables

Table 1. Relaxation Δd_{NN} of the NN-Cd atoms about V_{Te} (in percent of the bond length 2.81 Å of CdTe, a negative sign is indicating an inward relaxation), along with the relaxation energy ΔE_r , which is the energy lowering due to relaxation, and the calculated electric field gradient V_{zz} at a NN-Cd site ($\eta = 0$ due to symmetry).

	Δd_{NN} [%]	ΔE_r [eV]	V_{zz} [10^{21} V/m ²]
V_{Te}^0	-22	0.98	+2.0
V_{Te}^+	-2	0.05	+16.2
V_{Te}^{++}	+20	0.69	+24.6

Table 2. Experimental and theoretical values for the EFG caused by the Cd vacancy at the NNN-Cd site. V_{zz} values are given in units of 10^{21} V/m². The experimental error of V_{zz} and η is lower than $0.1 \cdot 10^{21}$ V/m² and 0.05, respectively.

	experiment ($T_M = 295$ K)			theory		
	EFG1	EFG2	EFG3	V_{Cd}^0	V_{Cd}^-	V_{Cd}^{--}
V_{zz}	± 3.0	± 5.1	± 5.6	-3.0	-4.1	-5.0
η	0.17	0.12	0.20	0.01	0.14	0.24

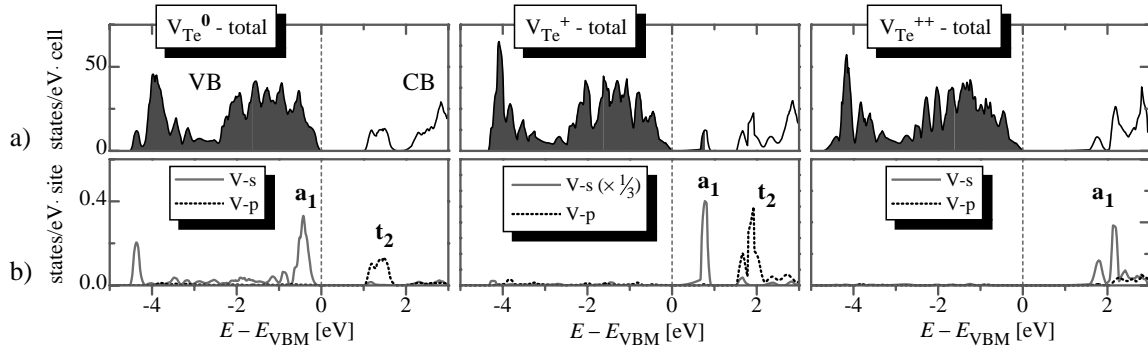


Fig. 1. (a) Total DOS for V_{Te}^0 , V_{Te}^+ , V_{Te}^{++} . Occupied states are shaded. (b) Local DOS at the vacancy site decomposed into s and p contributions. For V_{Te}^+ , the half filled a_1 level in the band gap is very narrow, therefore the s contribution needs a different scaling ($\times 1/3$) to be displayed.

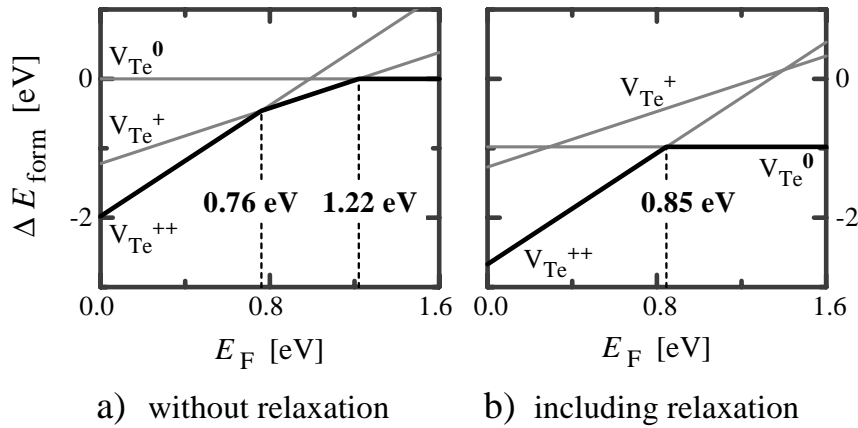


Fig. 2. Relative formation energies for the different charge states of V_{Te} as a function of E_F . (a) Relaxation suppressed. (b) Including relaxation. The left and the right margin of each plot corresponds to the VBM and the CBM, respectively; $\Delta E_{form} = 0$ corresponds to the unrelaxed configuration of V_{Te}^0 .